Available online at www.sciencedirect.com
ScienceDirect
Journal of Hazardous Materials 157 (2008) 277–285
Journal of Hazardous Materials
www.elsevier.com/locate/jhazmat

Biosorption of Cu(II) from aqueous solutions by mimosa tannin gel

İ. Ayhan Şengil [a,*], Mahmut Özacar [b]

[a] Department of Environmental Engineering, Engineering Faculty, Sakarya University, 54100 Sakarya, Turkey
[b] Department of Chemistry, Science & Arts Faculty, Sakarya University, 54100 Sakarya, Turkey

Received 6 October 2007; received in revised form 25 December 2007; accepted 28 December 2007
Available online 15 January 2008

Abstract

The biosorption of Cu(II) from aqueous solutions by mimosa tannin resin (MTR) was investigated as a function of particle size, initial pH, contact time and initial metal ion concentration. The aim of this study was to understand the mechanisms that govern copper removal and find a suitable equilibrium isotherm and kinetic model for the copper removal in a batch reactor. The experimental isotherm data were analysed using the Langmuir, Freundlich and Temkin equations. The equilibrium data fit well in the Langmiur isotherm. The experimental data were analysed using four sorption kinetic models – the pseudo-first- and second-order equations, and the Elovich and the intraparticle diffusion equation – to determine the best fit equation for the biosorption of copper ions onto mimosa tannin resin. Results show that the pseudo-second-order equation provides the best correlation for the biosorption process, whereas the Elovich equation also fits the experimental data well. Thermodynamic parameters such as the entropy change, enthalpy change and Gibb's free energy change were found out to be 153.0 J mol^{-1} K^{-1}, 42.09 kJ mol^{-1} and −2.47 kJ mol^{-1}, respectively.

Keywords: Mimosa tannin gel; Copper(II); Biosorption

1. Introduction

Copper is a very common substance that occurs naturally in the environment and spreads through the environment through natural phenomena. The production of copper has lifted over the last decades and due to this copper quantities in the environment have expanded. Copper is present in the wastewater of several industries, such as metal cleaning and plating baths, refineries, paper and pulp, fertilizer, and wood preservatives and it is highly toxic [1]. Most copper compounds will bound to natural organic materials and soil particles which will settle down to sediments. Soluble copper compounds form the largest threat to human health. Copper and its compounds are ubiquitous in the environment and thus copper is found frequently in surface water. Organization (WHO) recommended a maximum acceptable concentration of Cu^{2+} in drinking water of 1.5 mg L^{-1} [2]. Copper does not break down in the environment and because of that it can accumulate in plants and animals when it is found in soils. On copper-rich soils only a limited number of plants has a chance of survival. The excessive intake of copper by man leads to severe mucosal irritation, widespread capillary damage, hepatic and renal damage, central nervous problems followed by depression, gastrointestinal irritation, and possible necrotic changes in the liver and kidney [3].

The main techniques that have been used on copper content reduction from industrial waste are chemical precipitation, ion exchange, membrane filtration, electrolytic methods, reverse osmosis and solvent extraction. These conventional techniques can reduce metal ions, but they do not appear to be highly effective due to the limitations in the pH range as well as the high material and operational costs. Among these various treatment techniques, activated carbon adsorption is one of the most commonly used due to its high efficiency and easy operation [4,5].

In recent years, considerable attention has been focused on the removal of copper from aqueous solution using adsorbents derived from low-cost materials [6–8].

Tannins, natural biomass containing multiple adjacent hydroxyl groups and exhibiting specific affinity to metal ions, can probably be used as alternative, effective and efficient adsorbents for the recovery of metal ions. During the last years, the interest on biomaterials and specifically in tannins was growing.

* Corresponding author. Fax: +90 264 2955601.
E-mail address: asengil@sakarya.edu.tr (İ.A. Şengil).

0304-3894/$ – see front matter © 2008 Elsevier B.V. All rights reserved.
doi:10.1016/j.jhazmat.2007.12.115

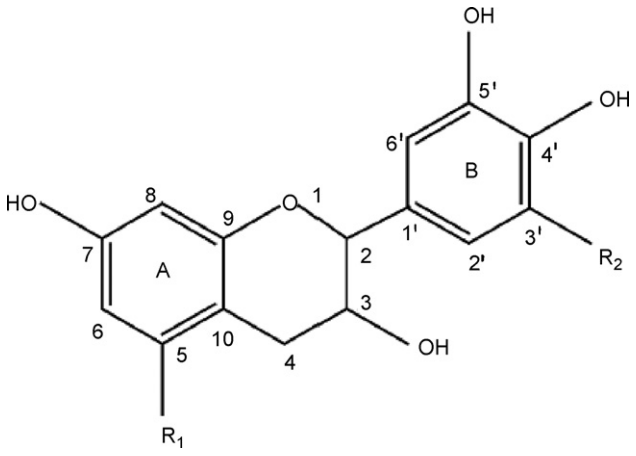

Fig. 1. The flavanoid unit in mimosa tannin. A-ring: R_1=H for resorcinol and R_1=OH for phloroglucinol; B-ring: R_2=H for pyrocatechol and R_2=OH for pyrogallol.

Tannins are an important class of secondary plant metabolites, water-soluble polyphenolic compounds of molecular weight ranged between 500 and some thousands Daltons. There are three kinds: hydrolizable, condensed and complex tannins [9]. However, tannins are water-soluble compounds, thus when they are used directly as an adsorbent for recovery of metals from aqueous systems, they have the disadvantage of being leached by water. To overcome this disadvantage, attempts have been made to immobilize tannins onto various water-insoluble matrices [10]. The chemical structures of condensed tannin are illustrated in Fig. 1.

The study on the removal of heavy metals from wastewater by tannin adsorbents was almost from the application of barks in the similar aspects. In 1977, Randall [11] observed that adsorption characteristics of barks for heavy metals rested on tannin structures present in the bark adsorbent. Later, researchers synthesized adsorbents from commercial tannins and applied them to remove heavy metals from wastewater, such as uranium [12], americium [13], chromium [14], copper [15], lead [16], thorium [17], gold [18] and palladium [19]. These studies illustrate that it is possible to remove heavy metals from wastewater with tannin adsorbents. The objective of this study is to systematically examine adsorption mechanisms, adsorption isotherms, adsorption kinetics and properties of a tannin gel adsorbent synthesized from mimosa tannin (MT) for removal of Cu^{2+} from aqueous solutions.

2. Materials and methods

2.1. Preparation of tannin gel particles

Eight grams of mimosa tannin powder, a kind of natural condensed tannins, was added to 50 mL of 13.3N aqueous NH_3 solution, followed by stirring for 5 min to dissolved it. To resulting solution was added 65 mL of formaldehyde (37 wt.%), followed by stirring at room temperature for 5 min for uniform mixing. When this stirring was stopped, a yellow precipitate formed. After the resulting liquid containing the precipitate was stirred for 30 min to complete cross-linking. The product was filtered through filter paper (Toyo Filter Paper No. 2). To the filtered precipitate was added 50 mL distilled water and the product was heated at 70 °C for 3 h. The mixture heated was collected by filtration. To the filtered precipitate was added 0.1N HNO_3 and was stirred for 30 min. The mixture was filtered through filter paper again. The precipitate obtained was allowed to stand at 80 °C to age it, thereby obtaining a tannin adsorbent consisting of an insoluble tannin [20]. The mimosa tannin resin (MTR) was prepared by grinding it in a laboratory type ball-mill. Then, it was sieved to obtain size fractions of −100 μm, +100 μm, +150 μm, +212 μm and +250 μm using ASTM Standard sieves. The Brunauer– Emmett–Teller (BET) surface area was measured from N_2 adsorption isotherms with a sorptiometer (Micromeriticis FlowSorbII-2300). The specific surface areas of different particle size of the tannin resin are given in Table 1.

Table 1
BET specific surface areas for the different tannin resin particle size ranges

Size fractions (μm)	BET surface area (m^2/g)
−100	13.56 ± 0.01
+100	13.05 ± 0.01
+150	12.50 ± 0.01

2.2. Proton titration experiment

The surface exchange capacity was measured by the proton exchange method [21]. The proton titration experiments were carried out to determine the number of valid sites for adsorption present on adsorbent particles. One hundred milliliters 0.1N NaOH solution; with 1.0 g particles were placed in well-sealed glass beaker and the beakers were placed on the thermostatic shaker. The shaking speed was 100 rpm and temperature was 20 °C. After 24 h, the solution in beaker was titrated by 0.1N HCl solution. The surface exchange capacity of the tannin resin was found to be 2.92 meq H^+ g^{-1}. The titration result suggests that the MTR surface is dominated by H^+ ion exchangeable groups that are largely –OH groups.

2.3. Batch adsorption experiment

A series of batch experiments were conducted to study the adsorption mechanism, adsorption isotherm and adsorption kinetics. Copper stock solution was prepared by dissolving $CuSO_4{\cdot}5H_2O$ (analytical reagent) in deionized water and further diluted to the concentrations required for the experiments. pH adjustment was fulfilled by adding HCl or NaOH into the solutions with known initial copper concentrations (10–150 mg L^{-1}).

In the determination of equilibrium biosorption isotherm, 0.1 g MTR and 100 mL of the desired concentration of Cu^{2+} solutions were transferred in 250 mL flask, and shaken on a horizontal bench shaker (Nüve SL 250) for 180 min (the time required for equilibrium to be reached between Cu^{2+} biosorbed and Cu^{2+} in solution) using a bath to control the temperature at 298 ± 2 K. The experiments were performed at 150 rpm.

At the end of the biosorption period, the samples (5 mL) were taken and centrifuged for 15 min at 5000 rpm and then analysed using AAS equipped with an autosampler (Shimadzu AA6701F). The amount of biosorption at equilibrium, Q_e (mg g^{-1}), was computed as follows:

$$Q_e = \frac{(C_0 - C_e)V}{W}$$

where C_0 and C_e are the initial and equilibrium solution concentrations (mg L^{-1}), respectively; V, the volume of the solution (L) and W, the weight of MTR used (g).

Batch kinetic biosorption studies were conducted in a temperature-controlled stirrer using 2000 mL of adsorbate solution and a fixed adsorbent dosage of 2.0 g. The stirring speed of the solution was fixed at 150 rpm for all batch experiments. The samples at different time intervals (5–180 min) were taken and at the end of each agitation period, the mixtures were centrifuged for 5 min. Then, the concentration of Cu^{2+} in the residual solution was analysed by means of atomic absorption spectrophotometry. The Cu^{2+} contents in all the experiments were determined at 327.4 nm analytical wavelengths by AAS equipped with an autosampler (Shimadzu AA6701F). The samples were read in duplicates. FTIR spectra were recorded on a Mattson Intensity Series FTIR spectrophotometer. The samples were prepared after removing the supernatant, and a portion of the residue was filtered through 0.45 μm Millipore membrane filters. The remaining portion was dried at 353 K for 4 h. Potassium bromide disks were prepared by mixing 1 mg of these samples with 200 mg of KBr (spectrometry grade) at 10,000 kg/cm^2 pressure for 30 min under vacuum. The spectra were recorded from 4000cm^{-1} to 400 cm^{-1} (100 scans) on samples in KBr disks. The effects of particle size, pH value, agitation rate, initial concentration and temperature on the adsorption capacity of MTR to Cu^{2+} were also investigated.

3. Results and discussion

3.1. Effect of particle size

A series of experiments have been carried out with a constant initial Cu^{2+} concentration of 100 mg L^{-1} and with various particle sizes of the mimosa tannin resin. Fig. 2 shows the experimental results obtained from series of experiments performed, using different tannin resin particle size ranges. The result shown in Fig. 2 indicates that the saturation capacity of Cu^{2+} adsorption by tannin resin was increased by decreasing the particle size. This behavior can be attributed to the relationship between the effective specific surface area of the adsorbent particles and their sizes. The effective surface area increased as the particle size decreased and as a consequence, the saturation capacity per unit mass of the adsorbent increased. This can be explained by the fact that for small particles a large external surface area is presented to Cu^{2+} in the solution which results in a lower driving force per unit surface area for mass transfer than when larger particles are used. Since C_0 is constant and the mass of tannin resin is constant, the external particle surface area increases as particle size decreases. Fig. 2 also shows that particle size has no significant effect on final adsorption (after 120 min).

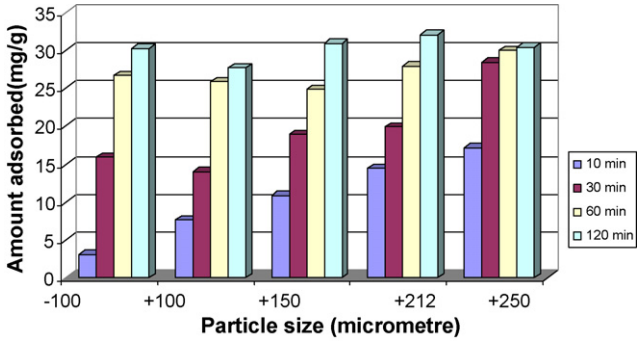

Fig. 2. Effect of particle size on adsorption of copper by mimosa tannin. Conditions: 100 mg L^{-1} concentration, 1 g L^{-1} dose, 298 K temperature, pH 4 and stirring speed 150 rpm.

3.2. Effect of pH

The uptake of Cu^{2+} was strongly affected by solution pH. At the initial Cu^{2+} concentration of 100 mg L^{-1}, copper removal efficiency was 8.2% at a solution pH of 2.0, but it increased sharply when solution pH rise from 2 to 4 (shown in Fig. 3), probably due to acidic dissociation of the phenolic hydroxyl groups of tannin, resulting in stronger complexing ability with metal ions. In low level of pH, H^+ ion will compete strongly with copper ions for the active sites, so adsorption was small. When the pH was increased, the competing effect of hydrogen ions decreased and consequently the metal uptake was increased. However, at higher pH values, Cu^{2+} would be precipitated and the phenolic hydroxyl groups of the tannin would more readily be oxidized, making it impractical to apply this approach above pH 8.0 [17].

3.3. Effect of contact time and initial concentration

Adsorption isotherms are usually determined under equilibrium conditions. A series of contact time experiments have been carried out with a constant initial Cu^{2+} concentration of various

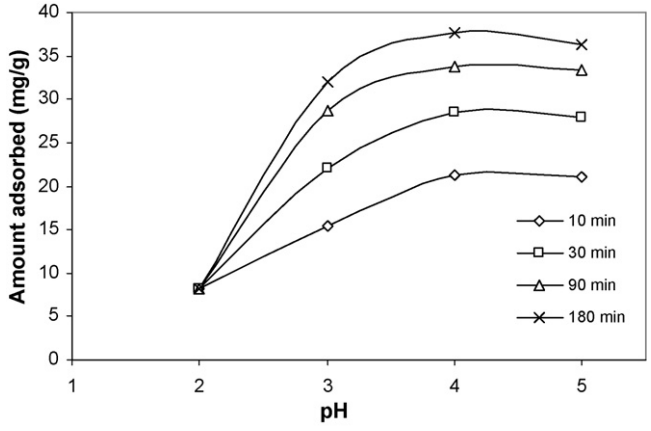

Fig. 3. Effect of pH on adsorption of copper by tannin resin. Conditions: 100 mg L^{-1} concentration, −100 μm particle size, 1 g L^{-1} dose, stirring speed 150 rpm and 298 K temperature.

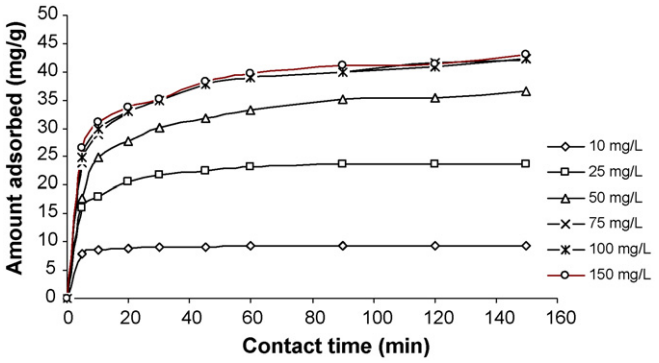

Fig. 4. Effect of contact time on adsorption of copper by mimosa tannin resin. Conditions: −100 μm particle size, 1 g L^{-1} dose, stirring speed 150 rpm, 298 K temperature and pH 5.

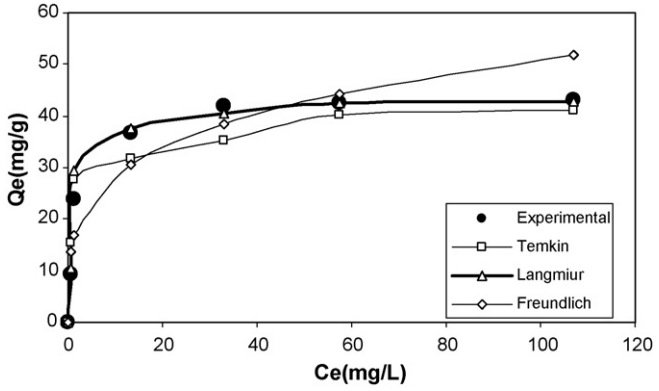

Fig. 5. Equilibrium isotherms of copper on MTR. Conditions: −100 μm particle size, 1 g L^{-1} dose, 298 K temperature and pH 5.

initial concentrations. Fig. 4 shows the contact time necessary for Cu^{2+} to reach saturation to be over 180 min. The distribution of Cu^{2+} between the tannin adsorbent and the Cu^{2+} solution, when the system is in a state equilibrium, is important to establish the capacity of the adsorbent for the Cu^{2+}. The initial concentration of Cu^{2+} has little influence of the time of contact necessary to reach equilibrium.

3.4. Equilibrium studies

Fig. 5 shows the equilibrium biosorption of copper (Q_e vs. C_e) using MTR. Equilibrium data, commonly known as sorption isotherms, are basic requirements for the design of sorption systems. Adsorption isotherm is important to describe how solutes interact with adsorbent. Therefore, to optimise the design of sorption system to remove heavy metals from effluents, it is important to establish the most appropriate correlation for the equilibrium curves. Three isotherm equations have been tested in the present study, namely, Langmuir, Freundlich and Temkin. The linear form of these isotherms [22,23] can be expressed by Eqs. (1)–(3), respectively:

$$\frac{C_e}{Q_e} = \frac{1}{K_L} + \frac{a_L}{K_L} C_e \quad (1)$$

$$\log Q_e = \log K_F + \frac{1}{n} \log C_e \quad (2)$$

$$q_e = B \ln A + B \ln C_e \quad (3)$$

where Q_e (mg g^{-1}) and C_e (mg L^{-1}) are the amount of adsorbed Cu^{2+} per unit weight of adsorbent and unadsorbed Cu^{2+} concentration in solution at equilibrium, respectively. The K_L and a_L are the Langmuir isotherm constants and the K_L/a_L gives the theoretical monolayer saturation capacity, Q_0. K_F is the Freundlich constant and $1/n$ the Freundlich exponent. A and B are the Temkin constants. The isotherm constants were determined from linear isotherm graphs for each of the isotherm equations tested. The values of the isotherm constants with the correlation coefficients are given in Table 2 for the copper–MTR system and the isotherms are plotted in Fig. 5 together with the experimental data points. The Langmuir equation represents the better fit of experimental data than the Freundlich and Temkin isotherm equation (Table 2).

In order to quantitatively compare the applicability of each isotherm, a standard deviation (S.D.) is calculated as follows [24]:

$$\text{S.D.} = \sqrt{\frac{\sum [(q_{e,exp} - q_{e,cal})/q_{e,exp}]^2}{(n-1)}} \quad (4)$$

where n is the number of data points. Table 2 lists the calculated results for each isotherm equation. Three isotherms were used to fit the experimental data. The comparison of the standard deviation of the isotherms should assist in identifying the best fit equation. Since the S.D. method represents the agreement between the experimental data points and models, the S.D. value provides a numerical value to interpret the goodness of fit of a given mathematical model to the data. Table 2 shows that the least values of S.D. are given by Langmuir isotherm.

3.5. Kinetic studies

Effects of contact time and initial copper concentration on biosorption of Cu^{2+} by MTR are shown in Fig. 4. The amount of Cu^{2+} biosorbed increased with increase in contact time and reached equilibrium after 180 min. The equilibrium time is independent of initial copper concentration. But in the first 30 min, the initial rate of biosorption was greater for higher initial copper concentration. Because the diffusion of copper ions through the

Table 2
Langmuir, Freundlich and Temkin isotherm constants

Langmuir					Freundlich				Temkin			
K_L (L/g)	a_L (L/mg)	Q_0 (mg g^{-1})	r^2	S.D.	K_F (mg g^{-1})/(mg L^{-1})$^{1/n}$	n	r^2	S.D.	B	A (L/g)	r^2	S.D.
24.39	0.56	43.71	0.999	0.1195	15.83	3.94	0.81	0.2756	6.13	18.91	0.92	0.3107

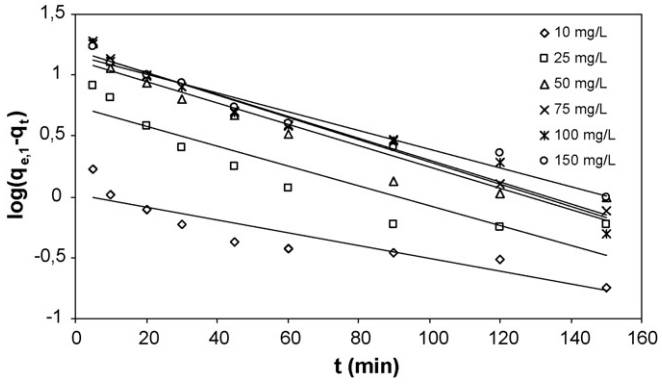

Fig. 6. Plot of the pseudo-first-order equation for the biosorption kinetics of copper on MTR at different initial concentrations.

solution to the surface of biosorbent is affected by the copper concentration, the mixing speed is constant. In order to examine the mechanism of biosorption process such as mass transfer and chemical reaction, a suitable kinetic model is needed to analyse the rate data.

The linear pseudo-first-order equation [25] is given as follows

$$\log(q_{e,1} - q_t) = \log q_{e,1} - \frac{k_1}{2.303}t \quad (5)$$

where q_t and $q_{e,1}$ are the amounts of Cu^{2+} adsorbed at time t and at equilibrium (mmol g^{-1}), respectively, and k_1 is the rate constant of pseudo-first-order adsorption process, (min^{-1}). Fig. 6 shows a plot of $\log(q_{e,1} - q_t)$ vs. t for biosorption of Cu^{2+} for the pseudo-first-order equation. The values of pseudo-first-order rate constants, k_1, and equilibrium biosorption capacities, $q_{e,1}$, for each initial copper concentration were calculated from slopes and intercepts of straight lines in Fig. 6. The values of pseudo-first-order equation parameters together with correlation coefficients are given in Table 3. The correlation coefficients for the pseudo-first-order equation obtained at all the studied concentrations were low. Also the theoretical $q_{e,1}$ values found from the pseudo-first-order equation did not give reasonable values. This suggests that this biosorption system is not a first-order reaction.

The linear pseudo-second-order equation [26,27] is given by

$$\frac{t}{q_t} = \frac{1}{k_2 q_{e,2}^2} + \frac{1}{q_{e,2}}t \quad (6)$$

where k_2 is the equilibrium rate constant of pseudo-second-order biosorption (g mg^{-1} min^{-1}). Fig. 7 shows typical plots of pseudo-second-order equation for the copper–MTR system as t/q_t vs. t. The straight lines in plot of linear pseudo-second-order equation show good agreement of experimental data with the pseudo-second-order kinetic model for different initial copper concentrations. The values of pseudo-second-order equation parameters together with correlation coefficients are listed in Table 3. The correlation coefficients for the pseudo-second-order equation were 0.999 for all concentrations. The calculated $q_{e,2}$ values also agree very well with the experimental data. This strongly suggests that the biosorption of Cu^{2+} onto MTR is

Table 3
Comparison of the first- and second-order equations, the intraparticle diffusion model and the Elovich equation rate constants, and calculated and experimental q_e values for different initial copper concentrations

C_0 (mg L^{-1})	$q_{e,exp}$ (mg g^{-1})	Pseudo-first-order equation			Pseudo-second-order Equation			Elovich equation			Intraparticle diffusion equation	
		k_1 (min^{-1})	$q_{e,cal}$ (mg g^{-1})	r^2	k_2 (g mg^{-1} min)	$q_{e,cal}$ (mg g^{-1})	r^2	α (mg g^{-1} min)	β (g/min)	r^2	k_{int} (mg g^{-1} $min^{1/2}$)	r^2
10	9.6	0.0122	11.22	0.84	0.05485	9.57	0.999	$7.58.10^7$	2.531	0.92	0.112	0.78
25	24.34	0.0186	25.34	0.85	0.01120	24.33	0.999	737.15	0.439	0.94	0.643	0.78
50	36.48	0.0202	38.41	0.92	0.00407	37.87	0.999	58.84	0.202	0.95	1.419	0.82
75	42.81	0.0207	43.85	0.97	0.00277	44.64	0.999	138.04	0.194	0.98	1.499	0.87
100	42.90	0.0211	44.26	0.95	0.00373	43.85	0.999	211.82	0.206	0.98	1.421	0.88
150	43.65	0.0177	46.24	0.96	0.00371	44.44	0.999	307.93	0.213	0.98	1.387	0.90

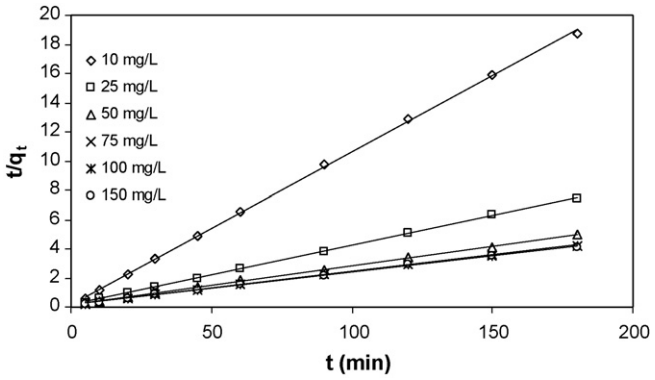

Fig. 7. Plot of the pseudo-second-order equation for the biosorption kinetics of copper on MTR at different initial concentrations.

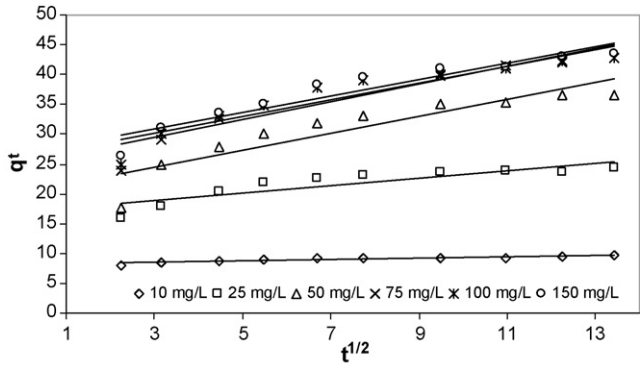

Fig. 9. Plot of the intraparticle diffusion equation for the biosorption of copper on MTR at different initial concentrations.

most appropriately represented by a pseudo-second-order rate process.

The adsorption data may also be analysed using the Elovich equation [28], which has the linear form:

$$q_t = \frac{1}{\beta}\ln(\alpha\beta) + \frac{1}{\beta}\ln t \quad (7)$$

where α is the initial sorption rate constant (mmol g^{-1} min^{-1}), and the parameter β is related to the extent of surface coverage and activation energy for chemisorption (g $mmol^{-1}$). Fig. 8 shows a plot of the Elovich equation for the same data. In this case, a linear relationship was obtained between Cu^{2+} biosorbed, q_t, and (ln t) over the whole biosorption period, with correlation coefficients between 0.68 and 0.96 for all the lines (Table 3). Also, Table 3 lists the kinetic constants obtained from the Elovich equation. In the case of using the Elovich equation, the correlation coefficients are lower than those of the pseudo-second-order equation. It cannot be used to describe the kinetics of biosorption of Cu^{2+} onto MTR.

Because Eqs. (5) and (7) cannot identify the diffusion mechanisms, the intraparticle diffusion model was also tested [29]. The initial rate of the intraparticle diffusion is the following:

$$q_t = k_{int} t^{1/2} \quad (8)$$

where k_{int} is the intraparticle diffusion rate constant, (mg g^{-1} $min^{-1/2}$). Such plots may present a multilinearity [29], indicating that two or more steps take place. The first, sharper portion is the external surface adsorption or instantaneous adsorption stage. The second portion is the gradual adsorption stage, where intraparticle diffusion is rate-controlled. The third portion is the final equilibrium stage where intraparticle diffusion starts to slow down due to extremely low adsorbate concentrations in the solution.

Fig. 9 shows a plot of the linearized form of the intraparticle diffusion model at all concentrations studied. As shown in Fig. 9, the external surface adsorption (stage 1) is absent. Stage 1 is completed before 5 min, and then the stage of intraparticle diffusion control (stage 2) is attained and continues from 5 min to 60 min. Finally, final equilibrium adsorption (stage 3) starts after 60 min. The copper is slowly transported *via* intraparticle diffusion into the particles and is finally retained in the micropores. In general, the slope of the line in stage 2 is called as intraparticle diffusion rate constant, k_{int}. The rate parameters, k_{int}, together with the correlation coefficients are also listed in Table 3.

A comparison of calculated and measured results for 100 mg L^{-1} Cu^{2+} concentration is shown in Fig. 10. As can be seen from Fig. 10, the pseudo-second-order equation provides the best correlation for all of the biosorption process, whereas the Elovich equation also fits the experimental data well. The pseudo-first-order equation and the intraparticle equation do not

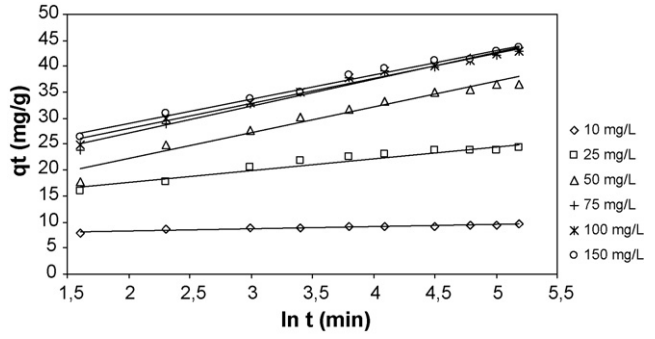

Fig. 8. Plot of the Elovich equation for the biosorption of copper on MTR at different initial concentrations.

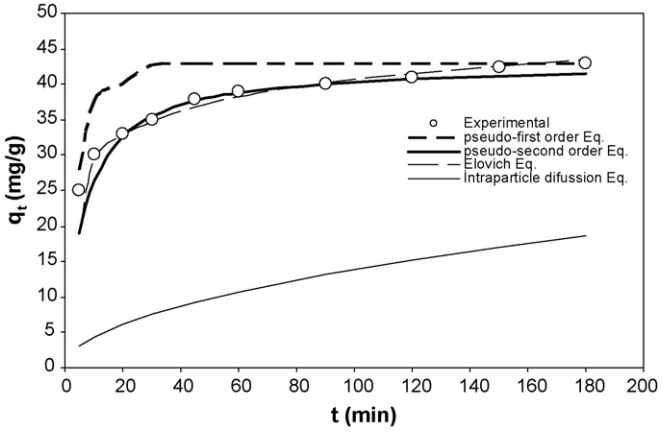

Fig. 10. Comparison between the measured and modelled time profiles for the biosorption of copper on MTR.

give good fits to the experimental data for the biosorption of Cu^{2+}. The Langmuir isotherm and pseudo-second-order kinetic model provide best correlation with the experimental data for the adsorption of copper ions onto MTR for different initial copper concentrations over the whole range studied. Both Langmuir isotherm and pseudo-second-order kinetic model assume that the MTR surface, containing the same reactive –OH groups such as pyrogallol groups binding copper ions, is homogenous and the operating adsorption mechanism is physical adsorption involving valency forces through sharing or exchange of electrons between copper and MTR. The homogenous surface of MTR provides multisites to the copper ions. Therefore, the pseudo-second-order equation, which was used in various molecules or ions chemisorption onto homogenous surface, can be fitted to the adsorption of copper ions very well [30,31].

When Cu^{2+} adsorption capacity of MTR was compared to that of some other sorbents reported in the literature, it was seen that the biosorption capacity of modified jute fibres, *Tectona grandis* L.f. leaves powder, H_3PO_4-activated rubber wood sawdust, cassava (Manihot sculenta Cranz) tuber bark, activated poplar sawdust and mimosa tannin gel for Cu^{2+} was 8.40 mg g^{-1}, 15.43 mg g^{-1}, 5.72 mg g^{-1}, 33.30–90.90 mg g^{-1}, 13.49 mg g^{-1} and 43.71 mg g^{-1}, respectively [32–36]. The results indicated that MTR have also good adsorption capacities for Cu^{2+}.

4. Thermodynamic studies

In order to determine thermodynamic parameters, experiments were carried out at different temperatures in the range of 298–353 K for Cu^{2+} adsorption. The thermodynamic parameters such as standard Gibb's free energy change (ΔG°), enthalpy change (ΔH°) and entropy change (ΔS°) were estimated to evaluate the feasibility and nature of the adsorption process [37]. The Gibb's free energy change, of the process is related to equilibrium constant by the equation

$$\Delta G^\circ = -RT \ln K_c \quad (9)$$

where, T is temperature in K, R ideal gas constant having value as 8.314 J mol^{-1} K^{-1} and K_c is thermodynamic equilibrium constant.

The thermodynamic equilibrium constant (K_c) of the adsorption is defined as:

$$K_c = \frac{C_\partial}{C_e} \quad (10)$$

where, C_a is mg of adsorbate adsorbed per liter and C_e is the equilibrium concentration of solution, mg L^{-1} [37]. According to thermodynamics, the Gibb's free energy change is also related to the enthalpy change (ΔH°) and entropy change (ΔS°) at constant temperature by the van't Hoff equation

$$\ln K_c = \frac{\Delta S^\circ}{R} - \frac{\Delta H^\circ}{RT} \quad (11)$$

The values of enthalpy change (ΔH°) and entropy change (ΔS°) were calculated from the slope and intercept of the plot $\ln K_c$ vs. $1/T$. The calculated values of thermodynamic parameters are reported in Table 4. A positive value of ΔH° as 42 kJ mol^{-1} for copper removal with MTR, indicated the endothermic nature of the process. A negative value of the free energy (ΔG°) (−2.47 kJ mol^{-1} at 298 K and −11.45 kJ mol^{-1} at 353 K), indicated the spontaneous nature of the adsorption process. It was also noted that the change in free energy, increases with increase in which exhibits an increase in adsorption with rise in temperature. This could be possibly because of activation of more sites on the surface of MTR with increase in temperature or that the energy of adsorption sites has an exponential distribution and a higher temperature enables the energy barrier of adsorption to be overcome.

Table 4
Thermodynamic parameters for the adsorption of Cu^{2+} by MTR*

Temperature (K)	K_c	ΔG° (kJ mol^{-1})	ΔH° (kJ mol^{-1})	ΔS° (J mol^{-1} K^{-1})
298	2.72	−2.47		
303	6.81	−4.83		
318	25.04	−8.51	42.09	153.0
338	28.23	−9.38		
353	49.50	−11.45		

* 50 mg L^{-1} concentration, pH 5, −100 μm particle size.

Generally for physical adsorption the free energy change (ΔG°) ranges from (−20 to 0) kJ mol^{-1} and for chemical adsorption it ranges between (−80 and −400) kJ mol^{-1}. The ΔG° for Cu(II) adsorption was in the range of (−2.47 to −11.45) kJ mol^{-1} and so the adsorption was predominantly physical adsorption [38]. A positive value of ΔS° as 153 J mol^{-1} K^{-1} showed increased randomness at solid solution interface during the adsorption of Cu^{2+} on MTR.

5. FTIR spectroscopy studies and adsorption mechanism

The FTIR spectra of MT, MTR resin, and Cu^{2+}-adsorbed MTR resin are shown in Fig. 11. Generally, wide bands in the

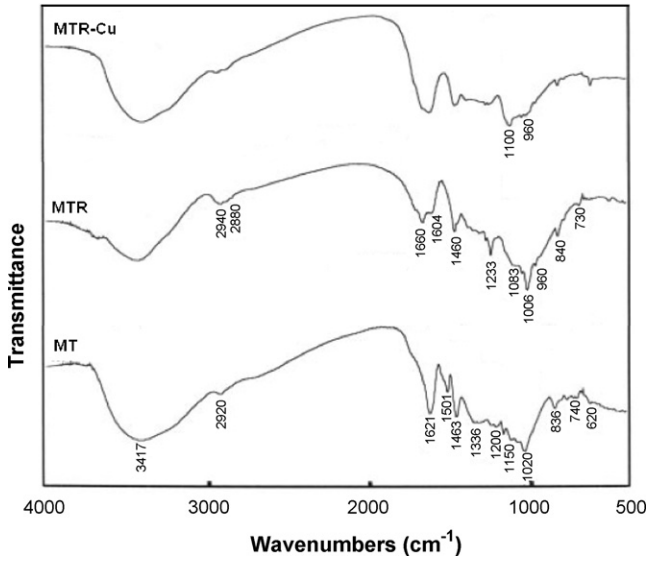

Fig. 11. FTIR spectra of metal ions adsorbed onto MTR. MT: mimosa tannin; MTR: mimosa tannin resin; MTR–Cu: Cu^{2+}-adsorbed mimosa tannin resin [33].

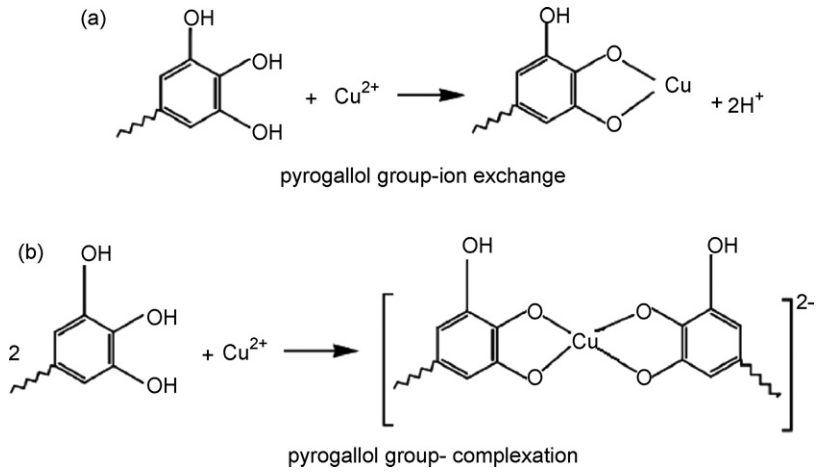

Fig. 12. Biosorption mechanisms for the biosorption of Cu^{2+} ion onto MTR. (a) Pyrogallol group-ion exchange. (b) Pyrogallol group- complexation.

range of 3550–3100 cm^{-1} correspond to –OH bridging groups in all systems and are attributed to water molecules hydrogen-bonded with –OH groups in the MTR particles. The small peaks in the region of 2880–2940 cm^{-1} are associated with the methylene ($–CH_2–$) bridges of the tannin resin. It has been demonstrated that a large number of methylene ether bridges ($–CH_2–O–CH_2–$) occur, which rearrange themselves with relative ease to form methylene (–CH2–) bridges with the release of formaldehyde. Also, C–H stretching vibrations in the benzene rings give absorption bands in this region. The absorption bands between 1621 cm^{-1} and 1463 cm^{-1} are characteristic of the elongation of the aromatic –C=C– bonds. The deformation vibration of the carbon–carbon bonds in the phenolic groups absorbs in the region of 1500–1400 cm^{-1}. The peak around 1250 cm^{-1} is associated with the –CO stretchings of the benzene ring and the dimethylene ether bridges formed by reaction with the formaldehyde. The peaks at 1100–1010 cm^{-1} in the spectrum of MT are due to C–O stretching and CH deformation.

The spectra of MTR resin were compared with the IR spectrum of the MT. The intensity of C–O peak at 1010 cm^{-1} is increased and broadened region of 1100–960 cm^{-1}. Also, the broad peaks in the spectra of MTR resin at this region may be attributed to the formation of dimethylene ether ($–CH_2–O–CH_2–$) linkage. Since the most characteristic absorption of aliphatic ethers is a strong band in the 1150–1085 cm^{-1} region due to asymmetrical C–O–C stretching, this band usually occurs near 1125 cm^{-1}. The deformation vibrations of the C–H bond in the benzene rings give absorption bands in the 840–730 cm^{-1} range. This group does not participate in any chemical reaction during the polymerization. However, this peak showed a gradual decrease as the process of polymerization progressed, because when the reaction takes place, the volume of the system contracts. The spectra of MTR–Cu^{2+}-adsorbed resins were compared with the IR spectra of the MT and MTR resin. The peak of methylol group (C–O) at the region of 1100–960 cm^{-1} in the spectra of MTR–Cu^{2+}-adsorbed resin is more broadened than those of MTR and MT spectra. These changes at MTR–Cu^{2+}-adsorbed resins are attributed to complexation of MTR resins and metal ions [39].

Mimosa tannin contains two different groups (catechol and pyrogallol) in B-ring for interacting with metals. The homogenous surfaces of MTR provide multisites to the metal ions. The mechanism by which metal ions are adsorbed onto different tannin resins has been a matter of considerable debate. Different studies have reached different conclusions. These include ion exchange, surface adsorption, chemisorption, complexation, and adsorption–complexation. In the case of ion exchange mechanism, metals react with adjacent phenolic groups of B-rings of the tannin resins to release protons with their anion sites to displace an existing metal. On the other hand, the hydroxyl groups in tannins offer special opportunities for the formation of metal complexes. Metals form complexes with phenolic groups with two adjacent hydroxyls (catechols), and the presence of a third adjacent hydroxyl (pyrogallols) increases the stability of the complexes [40,41].

We concluded that the biosorption mechanism migh be partly a result of the ion exchange or complexation between the Cu^{2+} ions and phenolic groups on MTR surfaces. Thus, the Cu^{2+} ions/tannin resins reaction may be represented in two ways as shown in Fig. 12 [39]. Adsorption yield at lower pH decreases due to ion exchange equlibrium. H^+ ions release during ion exchange process. Therefore at lower pH ion exchange equilibrium moves to the left.

6. Conclusion

The aim of this work was to find the possible use of mimosa tannin resin as a sorbent for the removal of Cu^{2+} from aqueous solutions. Experiments were performed as a function of particle size, initial pH, contact time, initial Cu^{2+} concentrations and temperature. Adsorption at pH 5 enhanced the efficiency of adsorption process, increasing in temperature from 298 K to 353 K lead to increase in adsorption yield. Adsorption equilibrium data were correlated with the Langmuir, Freundlich and Temkin isotherms and Langmiur model were found to provide the best fit of the experimental data. Assuming the batch adsorption as a single-staged equilibrium operation, the separation process can be mathematically defined using these isotherm con-

stants to estimate the residual concentration of Cu^{2+} or amount of adsorbent for desired purification. According to the Langmuir model, the maximum Cu^{2+} adsorption capacity of MTR was 43.71 mg g^{-1}.

The suitability of the pseudo-first-order, pseudo-second-order and particle-diffusion type kinetic models for the sorption of Cu^{2+} onto MTR for all situations was also discussed. The results showed that pseudo-second-order kinetic model was found to be in good agreement with the experimental results. Thermodynamic parameters of the adsorption confirmed the endothermic nature of sorption process as did the positive heat of enthalpy, accompanied by a positive value of entropy change. The standard Gibb's free energy change during adsorption process was negative, corresponding to feasible, spontaneous adsorption. Results obtained from this study showed that MTR can be used as an adsorbent for the removal of Cu^{2+} from the aqueous solution in a static batch system.

References

[1] M.H. Kalavathy, T. Karthikeyan, S. Rajgopal, L.R. Miranda, Kinetic and isotherm studies of Cu(II) adsorption onto H_3PO_4-activated rubber wood sawdust, J. Colloid Interface Sci. 292 (2005) 354–362.

[2] C.S. Rao, Environmental Pollution Control Engineering, Wiley Eastern, New Delhi, 1992.

[3] T. Gotoh, K. Matsushima, K. Kikuchi, Adsorption of Cu and Mn on covalently cross-linked alginate gel beads, Chemosphere 55 (2004) 57.

[4] S. Gomez-Salazar, J.S. Lee, J.C. Heydweiller, L.L. Tavlarides, Analysis of cadmium adsorption on novel organo-ceramic adsorbents with a thiol functionality, Ind. Eng. Chem. Res. 42 (2003) 3403.

[5] K.C. Justi, V.T. Fávere, M.C.M. Laranjeira, A. Neves, R.A. Peralta, "Kinetics and equilibrium adsorption of Cu(II), Cd(II), and Ni(II) ions by chitosan functionalized with 2[-bis-(pyridylmethyl)aminomethyl]-4-methyl-6-formylphenol", J. Colloid Interface Sci. 291 (2005) 369–374.

[6] M. Sarioglu, Ü.A. Atay, Y. Cebeci, "Removal of copper from aqueous solutions by phosphate rock", Desalination 181 (2005) 303–311.

[7] M. Horsfall Jr., A.A. Abia, A.I. Spi, Kinetic studies on the adsorption of Cd^{2+}, Cu^{2+} and Zn^{2+} ions from aqueous solutions by cassava (Manihot sculenta Cranz) tuber bark waste, Bioresour. Technol. 97 (2006) 283–291.

[8] Ö. Yavuz, Y. Altunkaynak, F. Güzel, Removal of copper, nickel, cobalt and manganese from aqueous solution by kaolinite, Water Res. 37 (2003) 948–952.

[9] E. Haslam, Plant Polyphenols-Vegetables and Tannins Revisited, Cambridge University Press, Cambridge, 1989.

[10] X. Liao, Z. Lu, M. Zhang, X. Liu, B. Shi, Adsorption of Cu(II) from aqueous solutions by tannins immobilized on collagen, J. Chem. Technol. Biotechnol. 79 (2004) 335–342.

[11] J.M. Randall, Variations in effectiveness of barks as scavengers for heavy metal ions, For. Prod. J. 27 (1977) 51–56.

[12] T. Sakaguchi, A. Nakajima, Accumulation of uranium by immobilized persimmon tannin, Sep. Sci. Technol. 29 (1994) 205–221.

[13] T. Matsumura, S. Usuda, Applicability of insoluble tannin to treatment of waste containing americium, J. Alloy Compd. 271–273 (1998) 244–247.

[14] Y. Nakano, K. Takeshita, T. Tsutsumi, Adsorption mechanism of hexavalent chromium by redox within condensed tannin gel, Water Res. 35 (2001) 496–500.

[15] H. Yamaguchi, R. Higasida, M. Higuchi, I. Sakata, Adsorption mechanism of heavy-metal ion by microspherical tannin resin, J. Appl. Polym. Sci. 45 (1992) 1463–1472.

[16] X.M. Zhan, X. Zhao, "Mechanism of lead adsorption from aqueous solutions using an adsorbent synthesized from natural condensed tannin", Water Res. 37 (2003) 3905–3912.

[17] X. Liao, L. Li, B. Shi, Adsorption recovery of thorium(IV) by Myrica rubra tannin and larch tannin immobilized onto collagen fibres, J. Radioanal. Nucl. Chem. 260 (2004) 619–625.

[18] T. Ogata, Y. Nakano, Mechanisms of gold recovery from aqueous solutions using a novel tannin gel adsorbent synthesized from natural condensed tannin, Water Res. 39 (2005) 4281–4286.

[19] Y.H. Kim, Y. Nakano, Adsorption mechanism of palladium by redox within condensed-tannin gel, Water Res. 39 (2005) 1324–1330.

[20] W. Shirato, Y. Kamei, Method of preparing insoluble hydrolysable tannin and method of treating waste liquid with the tannin, Us Patent, 5,300,677, 1994.

[21] Y. Al-Degs, M.A.M. Khraisheh, S.J. Allen, M.N.A. Ahmad, Sorption behavior of cationic and anionic dyes from aqueous solution on different types of activated carbons, Separ. Sci. Technol. 36 (2001) 91–102.

[22] M. Özacar, İ.A. Şengil, Equilibrium data and process design for adsorption of disperse dyes onto alunite, Environ. Geol. 45 (2004) 762–768.

[23] M. Özacar, Equilibrium and kinetic modelling of adsorption of phosphorus on calcined alunite, Adsorption 9 (2003) 125–132.

[24] F.C. Wu, R.L. Tseng, R.S. Juang, Kinetic modeling of liquid-phase adsorption of reactive dyes and metal ions on chitosan, Water Res. 35 (2001) 613–618.

[25] M. Özacar, İ.A. Şengil, Adsorption of reactive dyes on calcined alunite from aqueous solutions, J. Hazard. Mater. 98 (2003) 211–224.

[26] M. Özacar, İ.A. Şengil, 'Two-stage batch sorber design using second-order kinetic model for the sorption of metal complex dyes onto pine sawdust, Biochem. Eng. J. 21 (2004) 39–45.

[27] Y.S. Ho, G. McKay, Application of kinetic models to the sorption of copper(II) on to peat, Ads. Sci. Technol. 20 (2002) 795–817.

[28] M. Özacar, İ.A. Şengil, A kinetic study of metal complex dye sorption onto pine sawdust, Process Biochem. 40 (2005) 565–572.

[29] G. Annadurai, R.S. Juang, D.J. Lee, Use of cellulose-based wastes for adsorption of dyes from aqueous solutions, J. Hazard. Mater. 92 (2002) 263–274.

[30] M. Özacar, İ.A. Şengil, Adsorption of metal complex dyes from aqueous solutions by pine sawdust, Biores. Technol. 96 (2005) 791–795.

[31] C.W. Cheung, J.F. Porter, G. McKay, Sorption kinetics for the removal of copper and zinc from effluents using bone char, Sep. Purif. Technol. 19 (2000) 55–64.

[32] S.R. Shukla, R.S. Pai, Adsorption of Cu(II), Ni(II) and Zn(II) on modified jute fibres, Bioresour. Technol. 97 (2006) 1986–1993.

[33] Y. Prasanna Kumar, P. King, V.S.R.K. Prasad, Equilibrium and kinetic studies for the biosorption system of copper(II) ion from aqueous solution using *Tectona grandis* L.f. leaves powder, J. Hazard. Mater. B137 (2006) 1211–1217.

[34] M. Helen Kalavathy, T. Karthikeyan, S. Rajgopal, L.R. Miranda, Kinetic and isotherm studies of Cu(II) adsorption onto H_3PO_4-activated rubber wood sawdust, J. Colloid Interface Sci. 292 (2005) 354–362.

[35] M. Horsfall Jr., A.A. Abia, A.I. Spiff, Kinetic studies on the adsorption of Cd^{2+}, Cu^{2+} and Zn^{2+} ions from aqueous solutions by cassava (Manihot sculenta Cranz) tuber bark waste, Bioresour. Technol. 97 (2006) 283–291.

[36] F.N. Acar, Z. Eren, Removal of Cu(II) ions by activated poplar sawdust (Samsun Clone) from aqueous solutions, J. Hazard. Mater. B137 (2006) 909–914.

[37] V. Sarin, T.S. Singh, K.K. Pant, Thermodynamic and breakthrough column studies for the selective sorption of chromium from industrial effluent on activated eucalyptus bark, Bioresour. Technol. 97 (2006) 1986–1993.

[38] S. Debnath, U.C. Ghosh, Kinetics, isotherm and thermodynamics for Cr(III) and Cr(VI) adsorption from aqueous solutions by crystalline hydrous titanium oxide, J. Chem. Thermodynamics 40 (2008) 67–77.

[39] M. Özacar, C. Soykan, İ.A. Şengil, Studies on synthesis, characterization, and metal adsorption of mimosa and valonia tannin resins, J. Appl. Polym. Sci. 102 (2006) 786–797.

[40] L.J. Yu, S.S. Shukla, K.L. Dorris, A. Shukla, J.L. Margrave, Adsorption of chromium from aqueous solutions by maple sawdust, J. Hazard. Mater. B 100 (2003) 53–63.

[41] X.M. Zhan, X. Zhao, Mechanism of lead adsorption from aqueous solutions using an adsorbent synthesized from natural condensed tannin, Water Res. 37 (2003) 3905–3912.